Density functional methods for the magnetism of transition metals: SCAN in relation to other functionals

Yuhao Fu and David J. Singh*

Department of Physics and Astronomy, University of Missouri, Columbia, Missouri 65211-7010, USA

(Received 26 April 2019; revised manuscript received 23 June 2019; published 18 July 2019)

We report tests of various density functionals for ferromagnetic Fe, Co, and Ni with a focus on characterizing the behavior of the so-called strongly constrained and appropriately normed (SCAN) functional. It is found that SCAN is closer in behavior to functionals that yield localized behavior, such as hybrid functionals, than other semilocal functionals that are tested. The results are understood in terms of a tendency to differentiate orbitals, favoring integer occupation, which is necessary for a correct description of atomic systems, but inappropriate for the open shell metallic ferromagnetic metals studied here. Not only is the exchange splitting for open shells enhanced with SCAN, but also as seen in Ni, there is much more band dependence with significantly more overestimation for bands corresponding to the partially filled orbitals.

DOI: 10.1103/PhysRevB.100.045126

I. INTRODUCTION

The 3*d* transition metals and their compounds present an exceptional range of physical behavior, in part, because of the possibility for the 3*d* electrons to be localized, itinerant, or in between. Examples of this rich physics include the band-structure-related magnetism of elemental Fe, Co, and Ni, the Mott insulating physics of many transition-metal oxides, and the apparently distinct high-temperature superconductivity of cuprates and Fe pnictides. A long-standing goal has been the development of predictive theories and, in particular, computationally tractable theories that can reliably capture the physics of this range of materials. The challenge to theory is to develop density functionals that can describe both localized and itinerant behaviors in a predictive way. In this regard, the concept of "Jacob's ladder" has become widely held. In this view, adding more ingredients in density functionals and constraining this added flexibility by appropriate exact relations should give overall more accurate descriptions of atoms, molecules, and solids [1–3].

It has long been recognized that functionals, such as the local- (spin-) density approximation (LDA) and standard generalized gradient approximations (GGAs) do not provide an adequate treatment of correlated 3*d* oxides, such as the Mott insulating parents of the cuprate superconductors [4,5]. This is due to an inadequate treatment of correlations, which can be traced to self-interaction errors [6] and an insufficient tendency towards integer orbital occupations. This is the basis for methods that add a Hubbard U correction, i.e., LDA + U [7,8]. It is also a key aspect of a correct description of atoms and molecules where it can be traced to the need for a correct description of the exchange-correlation energy as a function of occupation number in order to avoid delocalization errors [9–11]. These delocalization errors can also be reduced by hybrid functionals, which can also correctly predict an antiferromagnetic insulating ground state for Mott insulators, including the high-T_c parent La_2CuO_4 [11–14]. These incorporate explicit orbital dependence and have been very important in the description of semiconductors where, in addition to improved ground-state properties, they also improve band gaps.

Recently, a semilocal meta-GGA functional, including the local (spin) densities, gradients, and a kinetic-energy density was proposed. This is the so-called strongly constrained and appropriately normed (SCAN) functional [15,16]. Advantages of this meta-GGA approach include the fact that calculations using a meta-GGA are computationally much less demanding than hybrid functional calculations for solids, the kinetic-energy density can provide information about orbital character, and calculations of energetics for diverse systems showed that the SCAN functional provides improvements over other functionals for a wide variety of solid-state and molecular properties [16–19]. Significantly, based on calculations, unlike GGAs, this functional is able to describe the ground state of La_2CuO_4, at least, qualitatively [20].

Thus, it is reasonable to suppose that the SCAN functional provides an overall improvement in the description of transition metals and compounds. However, recent results, especially for Fe, Co, and Ni, show this is not the case [19,21–23]. In particular, the magnetic tendency of these ferromagnetic metals is strongly overestimated as are the magnetic energies. This is particularly severe in the case of Fe. In that case, the large errors make the SCAN functional incapable of describing the phase stabilities underlying the materials science of steel [23].

Here, we compare SCAN with other functionals for these transition-metal ferromagnets. The results show the origin of the problems in the SCAN treatment of these materials is in the differentiation of orbitals. This is particularly seen in Ni where the exchange splitting is strongly enhanced, in particular, for bands corresponding to partially filled orbitals, leading to large errors for the band crossing the Fermi level at the X point, whereas enhancing the exchange splitting of

*singhdj@missouri.edu

occupied bands much more weakly. This is in contrast to standard semilocal functionals that give much more similar exchange splittings for the different bands. This underscores the difficulty of finding a functional that can treat the full range of transition-metal magnets. Such a functional must include the atomic physics favoring integer occupations in Mott insulators, such as undoped cuprates, and the tendency towards multiorbital open shell behavior materials that have significant itinerancy, such as Fe and Fe-based superconductors [24]. Thus, the problem of developing a functional that properly describes both localized electron behavior and itinerant behavior remains to be solved.

II. COMPUTATIONAL METHODS

We performed first-principles calculations with several different exchange-correlation functionals. These were the LDA, the Perdew-Burke-Ernzerhof (PBE) GGA [25], the SCAN [15], the Tao-Perdew-Staroverov-Scuseria (TPSS) [26], the revised TPSS (revTPSS) meta-GGAs [27,28], the Heyd-Scuseria-Ernzerhof (HSE)03 [29,30], the HSE06 [31], and the PBE0 [32,33] hybrid functionals. We additionally performed PBE + U calculations with various choices of the Hubbard parameter U.

We used two different methods, specifically, the projector augmented-wave (PAW) method as implemented in the VASP code [34,35], and the all-electron general potential linearized augmented plane-wave (LAPW) method [36] as implemented in the WIEN2K code [37]. Here, we focus on results at the experimental lattice parameters in order to better compare the description of magnetism in different approaches. These are $a = 2.860$ Å for bcc Fe, $a = 3.523$ Å for fcc Ni, and $a = 2.507$, $c = 4.070$ Å for hcp Co. The dependencies on the lattice parameter for Fe comparing the SCAN, the PBE, and the LDA were presented previously [23].

The VASP and WIEN2K codes have different implementations of the meta-GGA functionals, which involve different approximations. VASP implements self-consistent calculations but requires the use of PAW pseudopotentials, which are not available for the meta-GGA functionals. As such, we relied on PBE GGA based PAW pseudopotentials, which is an approximation. The general potential LAPW method, implemented in WIEN2K, is an all-electron method and does not use pseudopotentials. Additionally, WIEN2K has an efficient implementation of the fixed spin moment constrained density functional theory method [38,39]. This allows calculation of the magnetic energy as a function of the imposed magnetization, which provides additional information about the behavior of the functionals, and facilitates determination of the magnetic contribution to the energy. However, WIEN2K does not provide a self-consistent calculation with meta-GGA potentials, and, instead, the energy is calculated for densities obtained with the PBE GGA. This is an approximation for the energies and prevents calculation of the electronic band structures with the meta-GGA potentials. We find that the approximations above are not significant for the energies of the transition metals discussed here. A comparison of the different methods for Fe is presented in Table I.

In addition, as a test, we performed calculations for Fe using the ELK code [40]. This code has a self-consistent implementation of the SCAN functional. We obtain a spin magnetic for Fe of $2.64\mu_B$ with SCAN using this code. This is in excellent agreement with the VASP and WIEN2K results, supporting the accuracy of the present calculations.

TABLE I. Comparison of results for bcc Fe at the experimental lattice parameters using VASP and WIEN2K as employed here (see the text).

		LDA	PBE	SCAN
VASP	m_{sp} (μ_B)	2.15	2.25	2.65
	ΔE_{mag} (meV)	−411	−571	−1081
WIEN2K	m_{sp} (μ_B)	2.20	2.21	2.63
	ΔE_{mag} (meV)	−442	−561	−1114

The PAW calculations were performed with a plane-wave kinetic-energy cutoff of 400 eV. We used converged tested Brillouin zone samplings, based on uniform meshes. The LAPW calculations were performed with sphere radii of $R = 2.25$ bohr and basis sets defined by $RK_{max} = 9$, where K_{max} is the plane-wave sector cutoff. Local orbitals were used to treat semicore states. These are standard settings.

For the PBE + U calculations, we used different values of U with the standard procedure of Dudarev and co-workers [41] and the fully localized limit double counting. We covered the range up to $U = 8$ eV. It is common to find values in the range of $U = 5$ to $U = 8$ eV employed in literature for $3d$ transition-metal compounds. This is based, in part, on the view that U is a local atomic quantity that describes correlation effects that are missing in calculations with standard density functionals, such as the LDA or PBE GGA and, therefore, does not have much system dependence.

This view has been criticized, however, and procedures have been developed for determining U for particular systems. These are based on constrained calculations changing the electron occupation of the orbital of interest or by linear response [42,43]. This is important because screening, which strongly reduces U from its bare atomic value, varies from system to system. For our purpose, it is important to note that these methods for obtaining U are designed to improve the description of the energy variation between integer orbital occupations, i.e., line segments connecting the values at integer occupations.

In any case, we also estimated values of U using the linear-response method implemented in QUANTUM ESPRESSO. These estimated values are 4.33 eV for Fe, 2.62 eV for Co, and 5.56 eV for Ni. Although the basis set and implementation of PBE + U in the LAPW method and the pseudopotential plane-wave method of QUANTUM ESPRESSO are different so that values cannot be directly translated, these do provide an indication of the rough values, and we present calculations for these specific values. Importantly, these values are never zero, although, as discussed below, a value of zero gives the best agreement with experiment for these elemental transition-metal ferromagnets.

III. RESULTS AND DISCUSSION

We begin with bcc Fe. Figure 1 shows our results for the magnetic energy of bcc Fe with different exchange-correlation

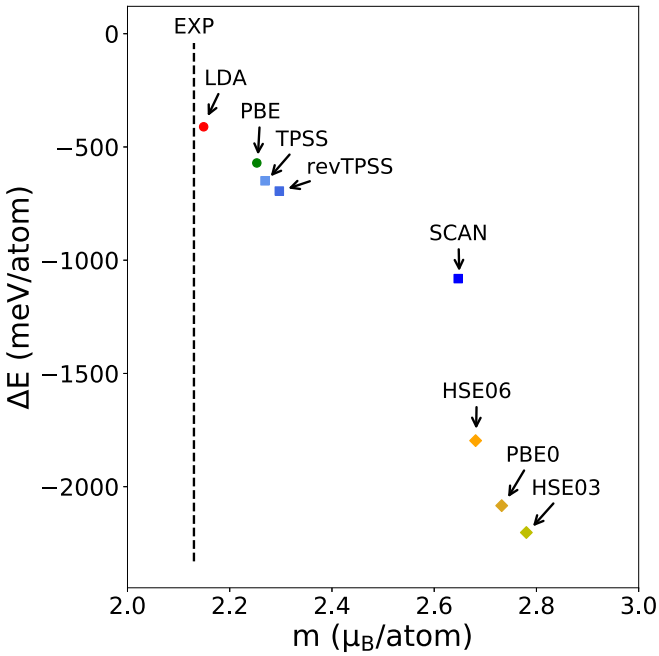

FIG. 1. The calculated magnetic energy and spin magnetizations of bcc Fe. The magnetic energy is defined as the difference in energy between the non-spin-polarized and ferromagnetic ground states. The calculations were performed self-consistently using VASP for the LDA, GGA, and meta-GGA functionals and WIEN2K for the hybrid functionals.

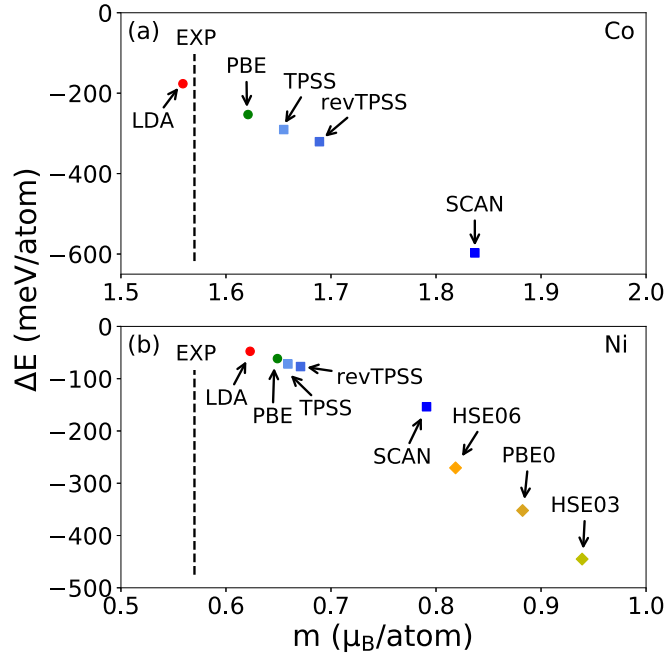

FIG. 2. Magnetic energy and spin magnetization per atom of hcp Co (top) and fcc Ni (bottom) as obtained with different functionals. The LDA, PBE GGA, and meta-GGA calculations were performed with VASP, and the hybrid functional calculations were performed with WIEN2K.

functionals at its experimental lattice parameter. Numerical values and magnetic moments are given in Table II.

The experimental spin magnetizations of Fe, Co, and Ni are $2.13\mu_B$, $1.57\mu_B$, and $0.57\mu_B$ per atom, respectively. As noted previously, the LDA and PBE GGA functionals provide values in good accord with experiment, whereas the SCAN meta-GGA was found to provide values significantly higher than experimental values [21,23]. This is why SCAN is unable to describe the phase balance that is central to the materials science of steel [23]. Furthermore, although the overestimates of the magnetization with SCAN amount to ∼25% for Fe, the magnetic energies were found to be greatly enhanced by factors of 2 or more in these metals. Moreover, as seen in Fig. 1, the SCAN meta-GGA behaves quite differently than the other meta-GGA functionals, TPSS, and revTPSS. Those functionals also enhance the magnetic tendency of Fe relative to the PBE GGA but to a much smaller extent than SCAN. This is consistent with the previously noted improved description of correlated materials using SCAN and underscores the difficulty of correctly describing both types of behavior with a single method.

It is also important to note that the already overestimated magnetic moments and energies with SCAN are further enhanced with hybrid functionals, which also describe the localized electron behavior of correlated oxides, including FeO [14,44–46]. This enhancement is both in terms of moments as was previously noted [47–49] and even more strongly in terms of magnetic energies.

We find similar results for Co and Ni. Spin magnetizations and magnetic energies are shown in Fig. 2. The main difference is that there is a greater relative overestimation of the moments with the TPSS and revTPSS meta-GGA functionals as compared to the PBE GGA.

As mentioned, another highly effective approach for localized systems is the addition of a Hubbard U correction as in the widely used LDA $+U$ and PBE $+U$ schemes. The correction is designed to better distinguish orbitals, favoring integer occupation, and, thus, correct delocalization errors in standard LDA and GGA calculations. In this sense, these

TABLE II. Properties of bcc Fe at its experimental lattice parameter (a_{exp}) and its calculated lattice parameter (a_{cal}).

	LDA	PBE	TPSS	revTPSS	SCAN	HSE06	PBE0	HSE03	Expt.
a_{cal} (Å)	2.75	2.83	2.80	2.80	2.84				2.86
m_{sp} (a_{exp}) (μ_B)	2.15	2.25	2.27	2.30	2.65	2.68	2.73	2.78	2.13
m_{sp} (a_{cal}) (μ_B)	1.93	2.20	2.15	2.16	2.57				
ΔE_{mag} (a_{exp}) (meV)	−411	−571	−650	−695	−1081	−1797	−2202	−2084	
ΔE_{mag} (a_{cal}) (meV)	−279	−528	−567	−598	−1028				

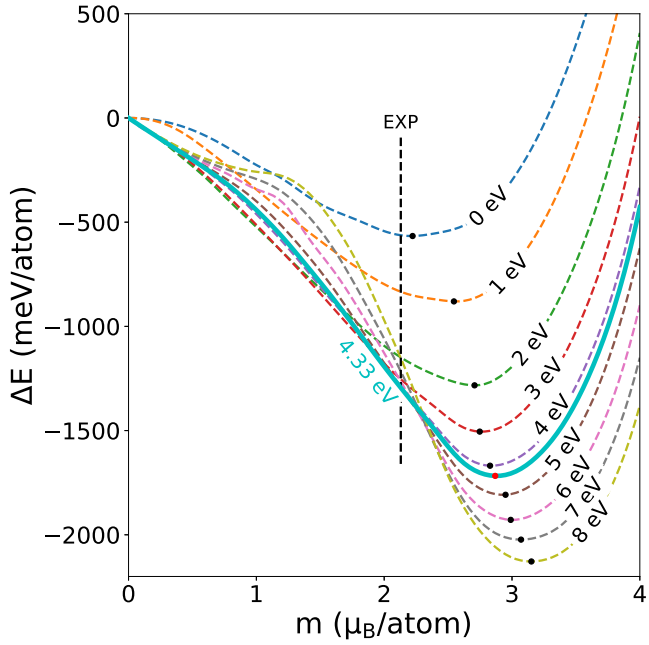

FIG. 3. Fixed spin moment energy as a function of spin magnetization per atom for bcc Fe as obtained with the PBE + U method implemented in WIEN2K.

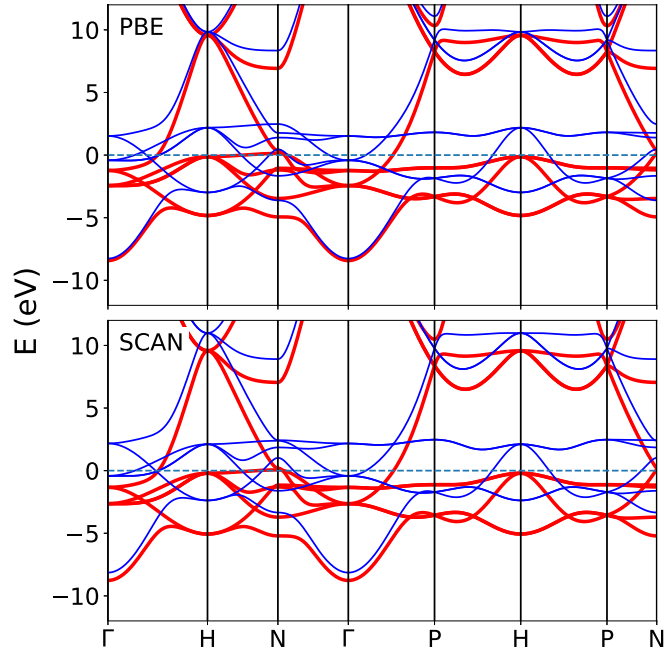

FIG. 5. Band structure of bcc Fe comparing PBE and SCAN as obtained from self-consistent calculations with VASP. The Fermi level is at 0 eV, and the majority (minority) spins are shown as heavy red (light blue).

Hubbard corrections have physics related to that of hybrid functionals, although with lower cost. As shown in Figs. 3 and 4, they do not improve results for magnetism in Fe, Co, and Ni. This had been noted previously for the moment of Fe by Cococcioni and de Gironcoli who found an overestimation by ∼20% in LDA + U calculations [43]. We find, here, that this overestimation is general and very strongly affects the magnetic energy.

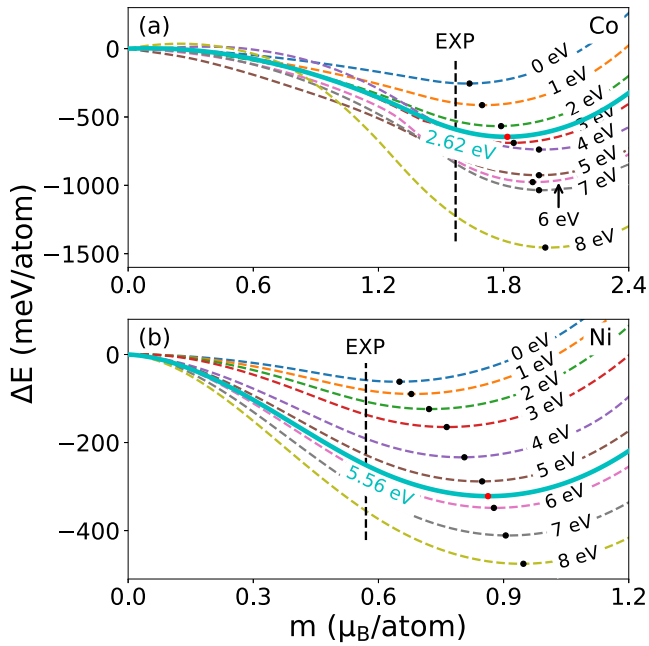

FIG. 4. Fixed spin moment energy as a function of spin magnetization per atom for Co and Ni as obtained with the PBE + U method implemented in WIEN2K.

It is important to note that PBE + U strongly degrades agreement with experiment for the values of U obtained from linear response and even for small values of U, e.g., 1 or 2 eV. Thus, the addition of a static Hubbard correction degrades agreement with experiment for these metals even if the correction is made small.

The Kohn-Sham eigenvalues in DFT do not correspond directly with experimental excitation energies, and, therefore, care should be taken in their interpretation. Nonetheless, within Kohn-Sham theory, they do control the occupancy of the Kohn-Sham orbitals and, therefore, the ground-state properties, such as energy and magnetization. For example, enhancing exchange splitting while keeping the bandwidth fixed will increase the magnetization. As such, analysis of the band structures can provide useful insight into the behavior of a functional.

It was observed that the d states of Fe are shifted to lower energy compared to the PBE GGA due to an increased exchange splitting, which disagrees with experiment [19,21]. This is closely connected with the larger magnetization since if the bands are relatively undistorted, the exchange splitting and magnetization will be closely related. Figures 5 and 6 show our band structures with PBE and SCAN for Fe and Ni. As noted by Ekholm and co-workers [21], the bandwidths using SCAN and PBE are similar, and the exchange splitting with SCAN is larger corresponding to larger magnetizations.

In addition to the overall exchange splitting, there are important differences between the PBE and the SCAN band structures, particularly, for Ni. The valence electronic structures of Fe and Ni can be roughly described as consisting

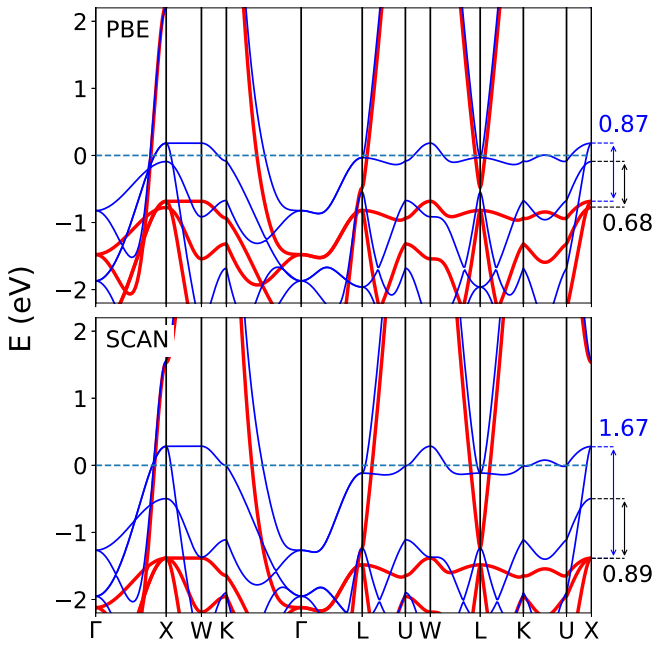

FIG. 6. Band structure of fcc Ni around the Fermi level comparing PBE and SCAN as obtained from self-consistent calculations with VASP. The Fermi level is at 0 eV, and the majority (minority) spins are shown as heavy red (light blue). The arrows and numerical values (in eV) give selected exchange splittings at the X point in eV. Note the similar exchange splittings for PBE and very different exchange splittings for SCAN.

of bands originating in the 4s orbital and the five 3d states. The lowest band at Γ originates from the s orbital and disperses rapidly upwards mixing with the d bands (note that a s band becomes p-like at the zone boundary where it is above the Fermi level in these elements). Thus, the lowest six bands consist approximately of the s band and the d band, which mix away from the Γ point. Figure 7 shows the exchange splittings of these bands for Fe and Ni at symmetry points. It has been previously noted that SCAN

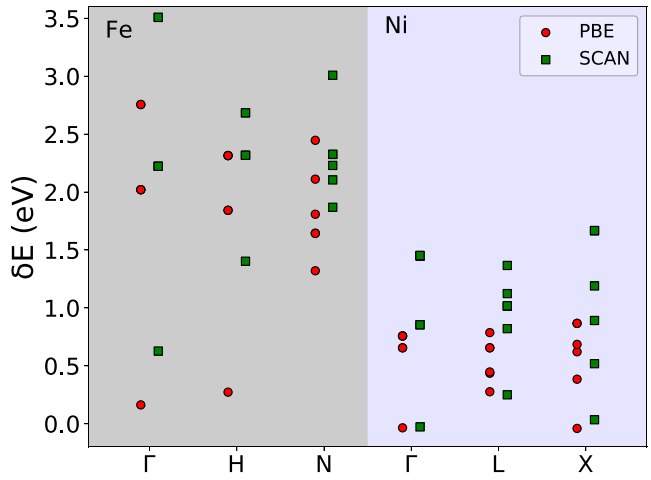

FIG. 7. Exchange splittings of the lowest six bands of bcc Fe and fcc Ni from the band structures of Figs. 5 and 6 at symmetry points.

yields enhanced exchange splittings relative to PBE, which then leads to enhanced moments [19,21]. Here, we find that this can be strongly orbital dependent, making the connection with the tendency of SCAN to favor integer occupation. This is important because a simple increase in exchange splitting is not enough to give reasonable results for strongly correlated oxides. This is because it will not, in itself, enhance band gaps if the highest occupied and lowest unoccupied bands are from the same spin. Therefore, orbital occupation dependence beyond a uniform enhancement of exchange splittings is an essential part of noted improvements in the treatment of strongly correlated systems.

In Fe, with the LDA and PBE functionals, the main d-band character is from ~ -5 to $+2$ eV relative to the Fermi energy E_F, the d-band occupancy is roughly seven electrons, there is partial filling of all the d orbitals, and the band structure agrees well with experiment aside from some renormalization of the low-energy bands as is well known [50–54]. It should be noted that an enhanced exchange splitting increases the energy separation of occupied and unoccupied d states, on average, which is a way for favoring integer orbital occupations.

In this regard, Mejia-Rodriguez and Trickey [55] recently presented an analysis of the SCAN functional in comparison with a so-called deorbitalized version. They find that an orbital-related parameter derived from kinetic-energy densities implies that SCAN favors spin-polarized states through enhanced exchange splittings [55]. We find that the situation is somewhat more complex because the exchange splitting is enhanced differently for different bands.

The electronic structure of ferromagnetic Ni has been extensively studied. It is roughly described as d bands and a partially filled s band with a d-band occupancy of roughly nine electrons. Differences between LDA and PBE calculations and experiment are well established in Ni. This includes a satellite feature observed in photoemission at ∼6 eV binding energy relative to the Fermi level [56], which, in any case, is a many-body effect that cannot be reproduced by Kohn-Sham eigenvalues. Additionally, Ni shows a considerably stronger renormalization of the d bands as compared with Fe [54, 57–59]. The d-band narrowing in Ni relative to LDA or PBE calculations is accompanied by a decrease in the exchange splitting. These two effects partially cancel as regards the spin magnetization so that, although the exchange splitting is overestimated by a factor of ∼2 in PBE calculations relative to experiment, the overestimate of the spin magnetization is only ∼10% ($0.63\mu_B$ in PBE vs $0.57\mu_B$ in experiment).

The electronic structure near the X point where an exchange split d band occurs near E_F has been extensively studied [54,57,58,60]. As seen in Fig. 6, the SCAN and PBE band structures are remarkably different in this region. In particular, the PBE band structure shows similar exchange splittings for the top d bands. The SCAN band structure, on the other hand, shows very different exchange splittings for the top bands. The partially filled top d band has an exchange splitting of 1.67 eV at X, whereas the next lower band is exchange split by 0.89 eV. As seen in Fig. 7, the SCAN functional produces a much larger range of exchange splittings in Ni than does the PBE functional. The largest exchange splittings are in the topmost partially filled d band. Thus, SCAN much more strongly differentiates the orbitals in Ni than PBE, again to the

effect of favoring integer occupancy through high exchange splittings of partially filled bands. The exchange splittings for fully occupied d bands are substantially smaller, which is a behavior different from PBE, for example, where the different d bands have much more similar exchange splittings. This feature of SCAN, which, as noted above, is important for the description of strongly correlated materials, degrades agreement with experiment for Ni.

IV. SUMMARY AND CONCLUSIONS

Calculations of the magnetic properties of Fe, Co, and Ni with various density functionals show that the SCAN functional is intermediate in accuracy between the standard PBE functional, which provides a generally good description of these materials, and approaches, such as PBE + U and hybrid functionals that provide a poor description of these ferromagnetic elements but can describe more localized systems, such as Mott insulators. SCAN is more different from the standard PBE than the earlier TPSS and revTPSS meta-GGA functionals and gives results in worse agreement with experiment for the magnetism of Fe, Co, and Ni.

The SCAN functional differentiates occupied from unoccupied states more strongly than PBE, which is manifested in larger exchange splittings in Fe and Ni and in the case of Ni in a greater difference in the exchange splittings between different bands. This can be understood as a greater tendency towards integer orbital occupation, which is an important ingredient in describing atomic systems and small molecules, and is a key aspect of strongly correlated materials, such as Mott insulators.

Thus, the challenge of developing a density functional approach that can reliably and predictively treat transition metals and their compounds, including both itinerant and localized systems, remains to be solved. This is an important problem not only from the point of view of physics, but also in the context of materials science. This is because, in materials science, the energies and resulting stabilities of different compounds and phases is important. However, at present, as shown by the present results functionals that describe all the different phases that may be important remain to be developed. For example, none of the practical functionals tested can give a good description of both metallic bcc and fcc Fe and, at the same time, Mott insulating oxides. It may be extremely challenging to solve this problem because it is unclear what semilocal information can be used to identify environments that lead to strong itinerancy from those that favor localization.

ACKNOWLEDGMENTS

We are grateful for helpful discussions with J. Sun, F. Tran, and S. Trickey. This work was supported by the U.S. Department of Energy, Office of Science, Basic Energy Sciences, Award No. DE-SC0019114.

[1] J. P. Perdew, A. Ruzsinszky, and J. Tao, J. Chem. Phys. **123**, 062201 (2005).
[2] S. Kummel and L. Kronik, Rev. Mod. Phys. **80**, 3 (2008).
[3] A. H. Romero and M. J. Verstraete, Eur. J. Phys. B **91**, 193 (2018).
[4] W. E. Pickett, Rev. Mod. Phys. **61**, 433 (1989).
[5] D. J. Singh and W. E. Pickett, Phys. Rev. B **44**, 7715 (1991).
[6] A. Svane, Phys. Rev. Lett. **68**, 1900 (1992).
[7] V. I. Anisimov, J. Zaanen, and O. K. Andersen, Phys. Rev. B **44**, 943 (1991).
[8] V. I. Anisimov, F. Aryasetiawan, and A. I. Lichtenstein, J. Phys.: Condens. Matter **9**, 767 (1997).
[9] A. J. Cohen, P. Mori-Sanchez, and W. Yang, Science **321**, 792 (2008).
[10] P. Mori-Sanchez, A. J. Cohen, and W. Yang, Phys. Rev. Lett. **102**, 066403 (2009).
[11] P. Rivero, I. de P.R. Moreira, and F. Illas, Phys. Rev. B **81**, 205123 (2010).
[12] R. L. Martin and F. Illas, Phys. Rev. Lett. **79**, 1539 (1997).
[13] X. Feng and N. M. Harrison, Phys. Rev. B **70**, 092402 (2004).
[14] J. K. Perry, J. Tahir-Kheli, and W. A. Goddard III, Phys. Rev. B **63**, 144510 (2001).
[15] J. Sun, A. Ruzsinszky, and J. P. Perdew, Phys. Rev. Lett. **115**, 036402 (2015).
[16] Y. Zhang, D. A. Kitchaev, J. Yang, T. Chen, S. T. Dacek, R. A. Samiento-Perez, M. A. L. Marques, H. Peng, G. Ceder, J. P. Perdew, and J. Sun, npj Comput. Mater. **4**, 9 (2018).
[17] J. Sun, R. C. Remsing, Y. Zhang, Z. Sun, A. Ruzzinszky, H. Peng, Z. Yang, A. Paul, U. Waghmare, X. Wu, M. L. Klein, and J. P. Perdew, Nat. Chem. **8**, 831 (2016).
[18] F. Tran, J. Stelzl, and P. Blaha, J. Chem. Phys. **144**, 204120 (2016).
[19] E. B. Isaacs and C. Wolverton, Phys. Rev. Mater. **2**, 063801 (2018).
[20] C. Lane, J. W. Furness, I. G. Buda, Y. Zhang, R. S. Markiewicz, B. Barbiellini, J. Sun, and A. Bansil, Phys. Rev. B **98**, 125140 (2018).
[21] M. Ekholm, D. Gambino, H. J. M. Jonsson, F. Tasnadi, B. Alling, and I. A. Abrikosov, Phys. Rev. B **98**, 094413 (2018).
[22] S. Jana, A. Patra, and P. Samal, J. Chem. Phys. **149**, 044120 (2018).
[23] Y. Fu and D. J. Singh, Phys. Rev. Lett. **121**, 207201 (2018).
[24] D. H. Lu, M. Yi, S. K. Mo, A. S. Erickson, J. Analytis, J. H. Chu, D. J. Singh, Z. Hussain, T. H. Geballe, I. R. Fisher, and Z. X. Shen, Nature (London) **455**, 81 (2008).
[25] J. P. Perdew, K. Burke, and M. Ernzerhof, Phys. Rev. Lett. **77**, 3865 (1996).
[26] J. Tao, J. P. Perdew, V. N. Staroverov, and G. E. Scuseria, Phys. Rev. Lett. **91**, 146401 (2003).
[27] J. P. Perdew, A. Ruzsinszky, G. I. Csonka, L. A. Constantin, and J. Sun, Phys. Rev. Lett. **103**, 026403 (2009).
[28] J. P. Perdew, A. Ruzsinszky, G. I. Csonka, L. A. Constantin, and J. Sun, Phys. Rev. Lett. **106**, 179902(E) (2011).
[29] J. Heyd, G. E. Scuseria, and M. Ernzerhof, J. Chem. Phys. **118**, 8207 (2003).
[30] J. Heyd, G. E. Scuseria, and M. Ernzerhof, J. Chem. Phys. **124**, 219906 (2006).
[31] A. V. Krukau, O. A. Vydrov, A. F. Izmaylov, and G. E. Scuseria, J. Chem. Phys. **125**, 224106 (2006).

[32] J. P. Perdew, M. Ernzerhof, and K. Burke, J. Chem. Phys. **105**, 9982 (1996).
[33] C. Adamo and V. Barone, J. Phys. Chem. **110**, 6158 (1999).
[34] G. Kresse and D. Joubert, Phys. Rev. B **59**, 1758 (1999).
[35] G. Kresse and J. Furthmüller, Phys. Rev. B **54**, 11169 (1996).
[36] D. J. Singh and L. Nordstrom, *Planewaves, Pseudopotentials, and the LAPW Method*, 2nd ed. (Springer, Berlin, 2006).
[37] P. Blaha, K. Schwarz, G. K. H. Madsen, D. Kvasnicka, and J. Luitz, WIEN2K, An augmented plane wave + local orbitals program for calculating crystal properties (2001).
[38] K. Schwarz and P. Mohn, J. Phys. F **14**, L129 (1984).
[39] V. L. Moruzzi, P. M. Marcus, K. Schwarz, and P. Mohn, Phys. Rev. B **34**, 1784 (1986).
[40] K. Dewhurst, http://elk.sourceforge.net/
[41] S. L. Dudarev, G. A. Botton, S. Y. Savrasov, C. J. Humphreys, and A. P. Sutton, Phys. Rev. B **57**, 1505 (1998).
[42] B. Himmetoglu, A. Floris, S. de Gironcoli, and M. Cococcioni, Int. J. Quantum Chem. **114**, 14 (2013).
[43] M. Cococcioni and S. de Gironcoli, Phys. Rev. B **71**, 035105 (2005).
[44] F. Tran, P. Blaha, K. Schwarz, and P. Novak, Phys. Rev. B **74**, 155108 (2006).
[45] M. Alfredsson, G. D. Price, C. R. A. Catlow, S. C. Parker, R. Orlando, and J. P. Brodholt, Phys. Rev. B **70**, 165111 (2004).
[46] A. D. Rowan, C. H. Patterson, and L. V. Gasparov, Phys. Rev. B **79**, 205103 (2009).
[47] J. Paier, M. Marsman, K. Hummer, G. Kresse, I. C. Gerber, and J. G. Angyan, J. Chem. Phys. **124**, 154709 (2006).
[48] Y. R. Jang and B. D. Yu, J. Phys. Soc. Jpn. **81**, 114715 (2012).
[49] P. Janthon, S. Luo, S. M. Kozlov, F. Vines, J. Limtrakul, D. G. Truhlar, and F. Illas, J. Chem. Theory Comput. **10**, 3832 (2014).
[50] J. Callaway and C. S. Wang, Phys. Rev. B **16**, 2095 (1977).
[51] B. Ackermann, R. Feder, and E. Tamura, J. Phys. F **14**, L173 (1984).
[52] A. Santoni and F. J. Himpsel, Phys. Rev. B **43**, 1305 (1991).
[53] J. Schafer, M. Hoinkis, E. Rotenberg, P. Blaha, and R. Claessen, Phys. Rev. B **72**, 155115 (2005).
[54] A. L. Walter, J. D. Riley, and O. Rader, New J. Phys. **12**, 013007 (2010).
[55] D. Mejía-Rodríguez and S. B. Trickey, Phys. Rev. B **100**, 041113(R) (2019).
[56] L. C. Davis, J. Appl. Phys. **59**, R25 (1986).
[57] D. E. Eastman, F. J. Himpsel, and J. A. Knapp, Phys. Rev. Lett. **40**, 1514 (1978).
[58] F. J. Himpsel, J. A. Knapp, and D. E. Eastman, Phys. Rev. B **19**, 2919 (1979).
[59] A. Liebsch, Phys. Rev. Lett. **43**, 1431 (1979).
[60] D. C. Tsui, Phys. Rev. **164**, 669 (1967).